Proceedings of the 28th IEEE
EMBS Annual International Conference
New York City, USA, Aug 30-Sept 3, 2006

Numerical Investigation of Blood Flow in a Sequential Aorto-Coronary Bypass Graft Model

Meena S, Dhanjoo N Ghista, Leok Poh Chua and Tan Yong Seng

Abstract— **Sequential grafting technique is adopted when one or more of the coronary arteries are blocked or severely narrowed. The objective of this study was to understand the influence of the anastomosis configuration on the blood flow in the three-dimensional coronary artery bypass graft (CABG) model. The finite volume technique was employed to model the 3-D blood flow pattern to determine the velocity and WSS distributions. This study presents the flow-field distributions of the velocity and WSS at two instances of the cardiac cycle, one during start of ejection (t=0.0 s) and the other during early diastole (t=0.32 s).**

Our results reveal that maximum wall shear stress was observed at the toe of the end-to side anstomosis. The smooth flow patterns observed in the side-to-side anastomosis region resulted in an almost uniform variation of WSS. The present work indicates that a side-to-side anastomosis would result in a better graft patency than an end-to-side anastomosis.

I. Introduction

THE sequential bypass grafting technique, first described by Flemma et al. [1] and Bartley [2] is a technique in which two or more coronary artery anastomoses are made with one single graft, usually the sapheneous vein. The advantages of this technique over the regular single graft technique include (i) lesser number of proximal anastomoses which result is reduction of operating time, (ii) an improved hemodynamic situation which in turn contributes to higher graft flow as reported by Grodin et al. [3] and Minale et al. [4]. Intraoperative studies [3] demonstrated a higher blood flow in the proximal segment of the sequential graft than in single coronary grafts. Higher patency rates were seen (through post angiograms) in the proximal (or side-to-side) anastomoses than in the distal (or end-to-side) anastomoses. These results were in agreement with that of Neill et al. [5] who confirmed that the proximal segment of the sequential graft has a higher velocity of blood flow than that seen in a single bypass graft.

Even though several numerical studies on CABG [6-7] have addressed important issues that relate to graft patency, all of them dealt with flow studies in a single bypass graft model (assuming only one portion of an artery to be occluded). Bonert et al. [8] compared the hemodynamic features (i) between diamond side-to-side and parallel side-to-side configuration and (ii) between proximal (side-to-side) anastomoses and distal (end-to-side) anastomoses. The objective of the present study was to use a somewhat realistic geometry and study the influence of the anastomosis configuration on the blood flow in an aorto-coronary bypass graft system.

Meena S was with Nanayng Technological University, Singapore 63 97 98. She is now with the Media Division, Institute for Infocomm Research, Singapore 119613 (phone no. 68742504; fax: 67755014; email: meena@i2r.a-star.edu.sg).

Dhanjoo N Ghista is with the Division of Bioengineering, Nanyang Technological University, Singapore 639798 (email: mdnghista@ntu.edu.sg)

Chua Leok Poh is with the School of Mechanical and Aerospace Engineering, Nanyang Technological University, Singapore 639798 (email: mlpchua@ntu.edu.sg)

Tan Yong Seng is with the National Heart Centre, Singapore 639798 (email: Tan_Yong_Seng@nhc.com.sg).

II. METHODOLOGY

A. Geometry Description

The dimensions of the various conduits, namely the aorta, the left main trunk of the coronary artery (LMCA), the branches of the LCA namely, the left anterior descending artery (LAD) and the left circumflex artery (LCx) with their branches, obtuse marginals OM1 and OM2 were obtained from Soulis et al. [9]. This data was based on experimental measurements that were previously reported by Dodge et al. [10]. As our prime interest was to understand the hemodynamic factors in the anastomosis region, only a small portion of the LAD was considered. The three-dimensional geometry of the aorto-coronary bypass graft model (Fig. 1) was constructed using the commercial fluid dynamic software **GAMBIT**. The sequential graft, namely the sapheneous vein employed in this study originates from the aorta at A and anastomosis to the 90% proximally occluded obtuse marginal (OM1) branch at B in a side-to-side anastomosis fashion and is then anastomed in an end-to-side fashion with the 80% proximally occluded obtuse marginal (OM2) branch at C. The intersection between the graft and the OM1 result in a

diamond shape while that between the graft and the LAD artery has an elliptical shape which is caused by the deformation of the larger diameter graft due to its sutured attachment to the smaller LAD vessel. Furthermore, we have used realistic graft-artery dimensions as provided by our surgeon co-author (TYS).

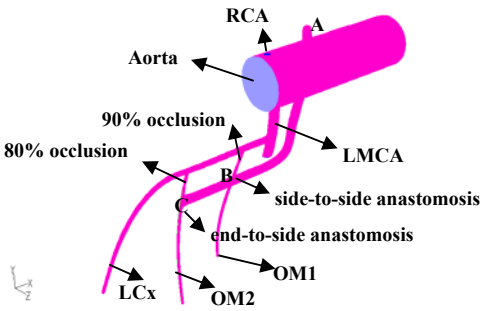

Figure 1 Geometry of the sequential aorto-coronary bypass graft model.

B. Model Properties and Flow conditions

The blood was assumed to be an incompressible, Newtonian fluid with a dynamic viscosity (μ) of 0.00408 Pa.s. The density (ρ) of blood was taken to be 1050 kg/m^3. The blood vessel walls were considered to be rigid and the no-slip conditions were applied at the walls. For a 3-D flow, the conservation of mass and linear momentum are expressed by the equations of continuity and Navier-Stokes, respectively, as:

$$\nabla . q = 0 \tag{1}$$

$$\rho\left(\frac{\partial q}{\partial t} + q.\nabla q\right) = -\nabla p + \mu \nabla^2 q \tag{2}$$

where p denotes the pressure and q denotes the velocity vector in three dimensions. The velocity distribution is obtained by solving the above equations subject to the input conditions given below.

The input conditions to the model are the measured time-varying flow-rate waveforms at the aorta entrance, LAD entrance, RCA entrance and the LCx reported from earlier works, Figs. 2(a)-(e). Moreover, based on Murray's law [11], the flow discharges were set analogous to the third power of the branching vessel diameter. The flow discharge values (as a percentage of the LCA inlet flow) at the various outlet branches of the LCA tree viz. LCx, OM1, OM2 and LAD are 22.44, 5.82, 15.4, 43.68 respectively.

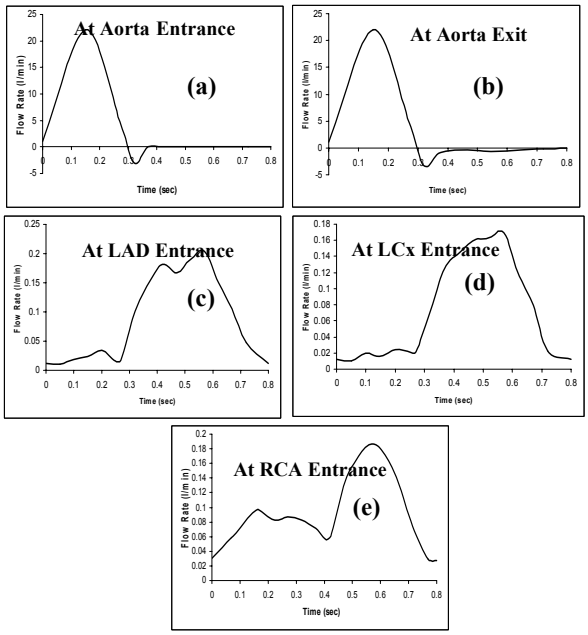

Figure 2 Flow-rate waveform at (a) inlet of the aorta, (b) aorta exit, (c) LAD entrance, (d) LCx artery and (e) RCA artery.

The fluid dynamics simulations are performed by using a control volume-based technique, implemented in the CFD code **FLUENT.** In the solution algorithm used by Fluent, the governing equations (conservation of mass and linear momentum) were solved sequentially. As the equations are non-linear (and coupled), several iterations of the solution loop were needed before a convergent solution was obtained. Using this approach, the resultant algebraic equations for the dependent variables (namely the velocities) in each control volume were solved sequentially by a point implicit (Gauss Seidel) linear equation solver in conjunction with an algebraic multi-grid (AMG) method. The governing equations were solved iteratively until convergence of all flow variables was achieved. The study was carried out by setting the convergence criteria as 10^{-5}. The typical computational time for one particular instant (t=0.32 sec) of the cardiac cycle was approximately 900 seconds on a desktop single processor (Pentium 1.75 Mhz, 1 GB RAM).

III. RESULTS AND DISCUSSION

The flow characteristics are analysed at two distinct time instances, namely the start of ejection (t=0.0 s) when blood flows from the left ventricle (LV) into the aorta and during early diastole (t=0.32 s) where there exists a small amount of back-flow into the left ventricle through the aortic inlet. To observe the velocity distribution of the entire flow field,

the computed velocity vectors are illustrated in the respective plane of symmetries of the conduits. The wall shear stress distributions are also illustrated for the above mentioned instances of the cardiac cycle. Due to the complex geometry and the out-of-plane nature of the model, the velocity vectors are shown in different regions of the computational domain, Figs. 3a- 3b.

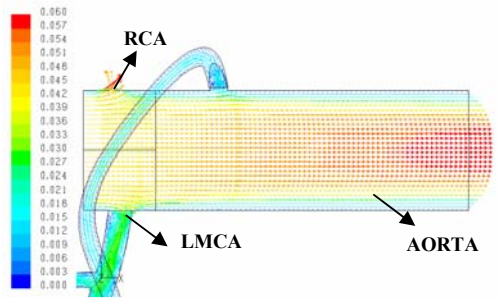

Figure 3a At t=0.0 s, velocity vectors in the aortic domain. There is very little flow entering the graft during systole.

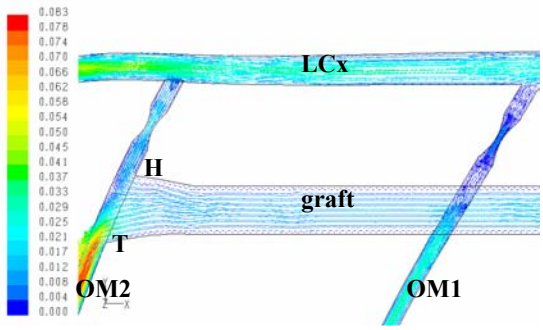

Figure 3b More flow is seen entering OM2 compared to OM1 artery. High velocities are observed at the toe of the end-to-side anastomosis. H-Heel, T-Toe.

Fig. 3a depicts the distribution of the velocity vectors in the aortic domain. The flow field in the aorta region appears to be like an inviscid flow. Even though there is very little flow entering the coronaries during the systole phase, it is noted that there is more flow in the RCA compared to the LCA. Most of the blood flows towards the ascending aorta leaving a small amount to perfuse the coronaries. Fig. 3b depicts the velocity vectors in the anastomosis regions. All the flow that enters the LCx proceeds downstream with increasing velocity due to tapering of the vessel except for a little amount which is seen to enter the branches, OM1 and OM2. As the proximal region of the OM1 is stenosed (90% stenosis), it is the blood that comes from the graft that perfuses the distal OM1. With regard to OM2 which is 80% stenosed, we observed that blood issuing from the graft moved in both directions, i.e, towards the proximal region of the OM2 and the distal part of OM2. High velocities were seen close to the toe region of the anastomosis.

The wall shear stress (WSS) is computed as a product of viscosity and the radial gradient of the velocity. Figs. 4a depict the contours of the WSS distribution in the entire domain. As the flow in the aortic domain was almost uniform the WSS is negligible. Maximum wall shear stress is seen at the distal end of the LCX which may be due to the tapering of the vessel. The side-to-side anastomosis experiences a low WSS compared to the end-to-side anastomosis which experiences a high WSS at the toe. This may be attributed to the geometry of the configuration. The proximal region of OM1 hardly experiences any WSS variation due to the negligible flow while the 80% stenosed proximal OM2 experiences a reasonable WSS, Fig. 4b.

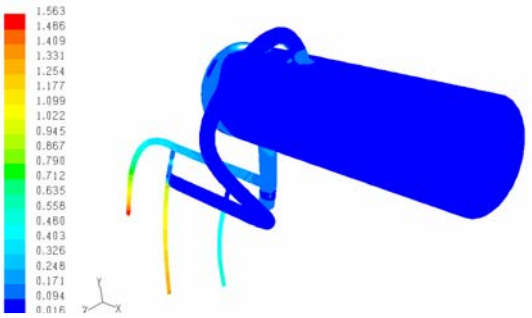

Figure 4a At t=0.0 s, the aorta experiences negligible WSS. Maximum magnitude of WSS is seen at the distal end of the LCx that arise due to steep velocity gradients

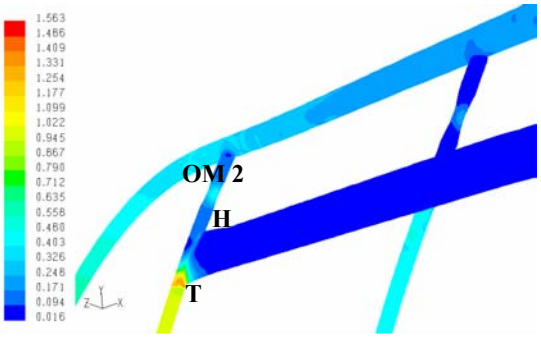

Figure 4b At t=0.0 s, the end-to-side anastomosis experiences a higher WSS variation compared to the side-to-side anastomosis. The magnitude of WSS at the toe is around 1.5 Pa. Flow disturbances seen at the proximal portion of OM2 results in a reasonable WSS (~0.45 Pa).

The flow field at the start of diastole is depicted in Fig. 5a-5b. The flow in the core region of the aorta is almost uniform with a velocity magnitude of 0.15m/s, Fig. 5a. The flow into the coronaries is higher compared to that observed during the systole phase. Even though the pattern remains qualitatively similar (except with a weak recirculation region seen at the proximal end of the OM1)

to that observed during start of ejection, the magnitude of velocity is high during the diastole phase thereby resulting in better perfusion of the coronaries, Fig. 5b. It was observed from the study that maximum perfusion occurs during the mid-diastole phase.

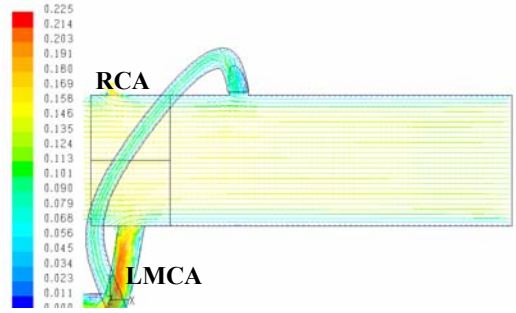

Figure 5a At the start of diastole t=0.32 s, flow in the core region of the aorta is almost uniform. More flow enters the LMCA compared to RCA.

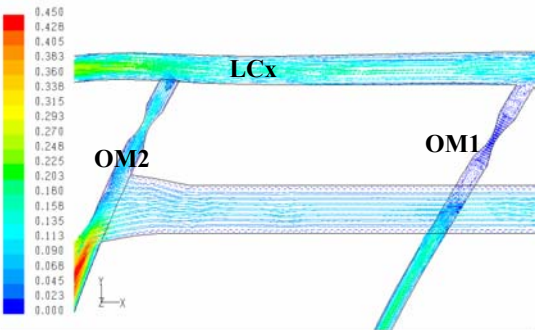

Figure 5b At t=0.32 s, the flow in the proximal portion of OM1 is almost stagnant while there is a reasonable amount of blood flowing through the constricted region in OM2 thus illustrating that OM2 is more perfused compared to OM1.

As most of the fluid flows into the coronaries, the WSS is almost negligible in the aortic domain, Fig. 6a. The smooth flow patterns seen around the side-to-side anastomosis results in a low WSS (around 3.5 Pa) while the toe region of the end-to-side anastomosis experiences a considerably high WSS of magnitude around 13 Pa, Fig. 6b. It may be due to the geometry that results in large velocity gradients. As seen in systole, the maximum WSS are also seen at the distal end of the LCx.

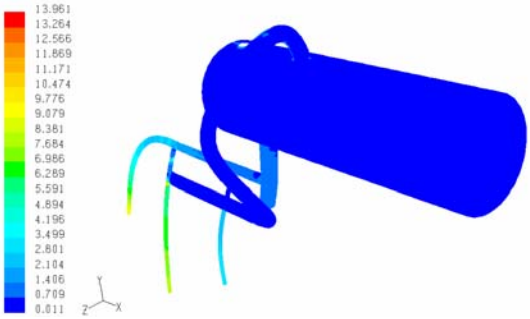

Figure 6a At t=0.32 s, the wall shear stress distribution in the entire computational domain.

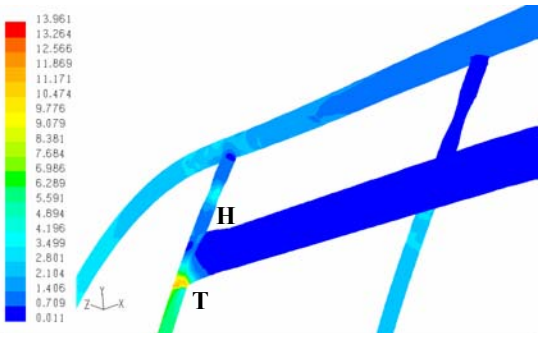

Figure 6b The WSS in the side-to-side anastomosis is around 4.5 Pa while that at the toe of the end-to-side anastomosis is around 13 Pa.

IV. Conclusion

The computed results have revealed that the side-to-side anstomoses contribute to safer hemodynamics thereby resulting in better graft patency than the end-to-side anastomosis.

References

[1] R. J. Flemma, W. D. Johnson, and D. Lepley, Jr., "Triple aorto-coronary vein bypass as treatment for coronary insufficiency", *Arch. Surg.*, 103, pp. 82-83, 1971.

[2] T. D. Bartley, J. C. Bigelow, and U. S. Page, "Aortocoronary bypass grafting with multiple sequential anastomoses to a single vein", *Arch. Surg.*, 105, pp. 915-917, 1972.

[3] C. M. Grondin, and R. Limet, "Sequential anastomoses in coronary artery grafting: technical aspects and early and late angiographic results", Annals of Thoracic Surgery, 23, pp. 1-8, 1977.

[4] C. Minale, N. P. Bourg, P. Bardos, and B. J. Messmer, "Flow characteristics in single and sequential aorto-coronary bypass grafts", *Journal of cardiovascular Surgery (Torino)",* 25, pp. 12-15, 1984.

[5] M. J. O'Neill, P. D. Wolf, T. K. O'Neill et al., "A rationale for the use of sequential coronary artery bypass grafts", *Journal of Thoracic and Cardiovascular Surgery*, 81, pp. 686-690, 1981.

[6] S. Meena, D. N. Ghista, L. P. Chua, Y. S. Tan, G. S. Kassab, "Analysis of Blood flow in an out-of-plane CABG model", *Am. J. Physiol. (Heart Circ. Physiol.)*, 29, pp. H283 - H295, 2006.

[7] M. H. Song, S. Masaru, U. Yuichi, "three-dimensional simulation of coronary artery bypass grafting with the use of computational fluid dynamics", *Surgery Today*, 30, pp. 993-998, 2000.

[8] M. Bonert, J. G. Myers, S. Fremes, J. Williams, and C. R. Ethier, "A numerical study of blood flow in coronary artery bypass graft side-to-side anastomoses", *Annals of Biomedical Engineering*, 30, pp. 599-611, 2002.

[9] J. V. Soulis, T. M. Farmakis, G. D. Giannoglou, and G. E. Louridas, " Wall shear stress in normal left coronary artery tree", *Journal of Biomechanics*, 39(4), pp. 742-749, 2006.

[10] J. T. Dodge Jr., B. G. Brown, E. L. Bolson, and H. T. Dodge, "Intrathoracic spatial location of specified coronary segments on the normal heart. Applications in quantitative arteriography, assessment of regional risk and contraction, and anatomic display", *Circulation*, 78, pp. 1167-1180, 1988.

[11] C. D. Murray, "The physiological principle of minimum work. I. The vascular system and the cost of blood volume", *Proceedings of National Academy of Science*, 12, , pp. 207-214, 1926.